

WET-CHEMICAL SYNTHETIZATION TO CNT-HEMATITE NANOCOMPOSITES AND CHARACTERIZATION

Danish Raza^{*1}, Adil², Syed Farhan Hasany³, Sajid Hussain⁴

^{*1,2} Department of Physics, NED University of Engineering & Technology, Karachi, Pakistan.

³Department of Chemistry, NED University of Engineering & Technology, Karachi, Pakistan.

⁴Institute of Industrial Electronics Engineering, Karachi, Pakistan.

^{*1}danishraaza@yahoo.com

DOI: <https://doi.org/10.5281/zenodo.19808137>

Keywords

Article History

Received: 28 February 2026

Accepted: 07 April 2026

Published: 27 April 2026

Copyright @Author

Corresponding Author: *

Danish Raza

Abstract

Since a few decades, various types of nanomaterials differing in size, shape, composition, morphology and structure have been synthesized by distinct techniques and modifications. Also, they were characterized to explore their chemical, physical, electrical and magnetic insights. The synthetic route employed has crucially effects on the properties of synthesized nanoparticle. Carbon nanotubes (CNT) is unique, among other nanomaterials, in its ability to be doped by another elements or compound, to obtain the features and characteristics, as per desired, in synthesizing nanocomposites and then implementing to a specific application. This study was a step to synthesis a nanocomposite that consisting hematite on the surface of CNT by wet chemical approach, which is simple, low cost, non-toxic and accessible easily in a laboratory. Further, the synthesized nanoparticle was characterized by XRD, FTIR, SEM and VSM. It implies that CNT-Hematite found in the synthesized nanostructure with some contaminations and it is a less ferromagnetic material in nature. At room temperature it shows the saturation magnetization, remnant magnetization and coercivity ~ 1.2 emu/g, 0.5 emu/g and 200 Oersted respectively, in compliance to be a suitable and contrivance candidate for lithium-ion battery or super capacitors' applications.

1. INTRODUCTION

Metal oxide nanoparticles have been growing excessive importance in wide-scale applications in sensor technology[1], light emitting devices[2], Lithium Ion battery[3] and click catalysis[4]. The preparation method plays a key role in determining the particle size and shape, size distribution, surface chemistry and therefore to be conformed to its applications. In comparison to other expensive ways, Wet Chemical synthesis is simple and direct to get the desired nanoparticles with having good control, up to an extent, over the size, shape, phase and reaction conditions [5]. It

was mostly used in preparing various size nanoparticles than the Chemical Vapor decomposition, Electrochemical, reverse micelle and sol-gel techniques. Additionally, In this route, the concentration of cations/anion and PH value effect on the size and structure of the nanoparticles. However, agglomeration, which can be reduced by coating or adding dispersing agent and the wide distribution of nanoparticles in size make it limited in use. Nanoparticles of Au, Ag, Pt, Pd were prepared by reduction with a suitable stabilizing agent[6]. And the capping agent has been used as reducing agent, for instance:

Turkevich established gold nanoparticles [7], Han et al prepared the gold nanoparticles in the non-aqueous medium, formamide, as reducing agent [8]. Brust et al. obtained gold particles in the organic solvent, thiol, as a stabilizing agent [9] and further, Silver nanoparticles obtained by using Silane, as capping agent [10]. For the synthesis of metallic nanoparticles at low temperature and inert atmosphere, alkaline and electrode reagents were used in the presence of complexing agents [11], [12]. Bonnemann et al. reported that stabilization of nanoparticles of colloids could be produced by using organoaluminum compounds that control the growth of particles and thus, it opened the choice of using heterogeneous catalyst [13], [14]. The same author extended the usage of organoaluminum catalyst to include metal carbonyl decomposition route [15], and observed that the size of nanoparticles depends upon the temperature and the molar ratio between the ions. Polyols acting as a stabilizer or reducing agent produced monodispersed nanoparticles [16]. Reduction of metals at the cathode and the dissolution of metal occurred at the anode to attain precipitation with an addition of a suitable stabilizer. Pd, Au and Fe monodispersed nanoparticles which synthesized by this electrochemical reduction [17]. And it was observed that the particle size decreased when increased the current density in the electrochemical solution [18], [19]. Metal oxide nanoparticles obtained, using hydroxide and calcinated coprecipitation, were $\text{Ni}_0.5\text{Zn}_0.5\text{Fe}_2\text{O}_4$ and MgFe_2O_4 spinel structure in the presence of NaOH at calcinated temperature 300°C or above [57], [58]. In some cases for a simple TiO_2 binary oxide, crystalline oxide precipitated without calcination [59] while some other route requires calcination to occur between 50°C and 100°C [60]. Influenced by surfactants, co-surfactants, reacting phases and reaction condition, Micro emulsion, a better way, to produce uniform size particles, however, remaining of surfactant and size scaling of nanoparticles are drawbacks of this route. Sol gel method is used to produce a large variety of metal oxide nanoparticles from its salts under ambient temperature and heat treatment. Nature and

concentration of solvents, reaction temperature, PH value and aging are the crucial parameters to control nucleation and growth. While, it is limited to be employed for individual nanoparticles.

For industrial purpose, scaling up the mass of nanoparticles is mandatory to achieve good quality and if increased the amount of volume, it suffers variation in nucleation and growth rate and thereby size of the product. To overcome the issue, flow synthesis in low dimension preferred to increase mass rate and time rate due to rapid mixing and high interfacial area and thus the size of the particle as well as the nucleation and growth rates can be controlled via reactor dimension, concentration, mixing and temperature [20].

2. Materials and Methods

The MWCNT was activated by stirring with 1M solution of HNO_3 for 6 hours followed by filtering, washing with distilled water and drying at 100°C . The process repeated three times to get purified MWCNT. 4g of $\text{Fe}(\text{NO}_3)_3$ are stirred for one hour under Nitrogen environment with the addition of 8 mL of NH_4OH followed by purging N_2 gas in the solution. Further, ammonium hydroxide was added drop wise to achieve the supersaturated solution and Nitrogen bubbled water was also poured with high stirring for 30 min and as a product Hematite obtained. The mixture of 100 gm of Multi-wall CNT and 500 mg of $\text{Fe}(\text{NO}_3)_3 \cdot 9\text{H}_2\text{O}$ were stirred for 30 minutes in the presence of Nitrogen environment. Having 1:10 molar ratio of NH_4OH and distilled water also added in the solution. The solution was washed using a centrifuge with distilled water and then alcohol three times each. Heat treatment was given to the sample at 350°C for 30 min consequently, nanocomposite formed.

3. Results and discussion

3.1 XRD

The XRD analysis of the synthesized composite was performed by XRD diffractometer (XPERTPRO) with $\text{Cu K}\alpha$ having a wavelength ($\lambda = 1.5406 \text{ \AA}$) operated at 30 mA and 40 kV and is presented in figure 4.1, where vertical lines are shown as reference data indexed (COD:901-2231) and (COD:101-1241) both for CNT and

hematite. The synthesized composite could be indexed either for multi-wall CNT or Hematite and also many peaks were in the XRD

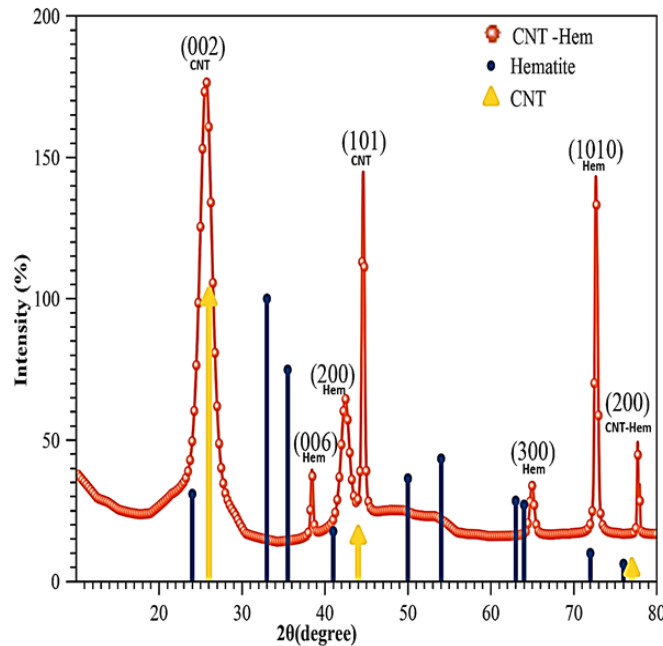


Figure 1: XRD Spectrum with CNT-Hematite Peaks

spectrum which told it is a nano hydride[21]. It could be seen that Peaks on the 26°, 44.5°, 77° degrees signifying the cylindrical and multi walls nature of graphene sheets having interlayer spacing 0.34 nm, 0.20 nm and 0.121 nm respectively which confirms that CNT existence[22] (P4132, ICDD: 391346) while remaining peaks at 42°, 38°, 65°, 73°, 78° corresponding to 0.234 nm, 0.213 nm, 0.143 nm and 0.130 nm ensure the presence of hexagonal

hematite (P4132, ICDD: 391346). The average crystallite size depends upon the synthetic method employed which in the synthesized composite found 0.457 nm by using Debye-Scherrer formula $D = 0.9\lambda / \beta \cos\theta$ where 'λ' is the wavelength used (0.154 nm), 'β' is the angular line width at half maximum intensity in radians and 'θ' is the Bragg's angle. From XRD the parameters obtained with 2θ and intensity are shown in table. 1

Table 1: XRD Parameters with 2θ and average crystal size

2θ (degree)	38.397	44.573	64.912	72.648
FWHM (radian)	0.0051	0.0060	0.0103	0.0051
D Spacing (nm)	0.2344	0.2032	0.1436	0.1301
Intensity (%)	15.28	80.32	11.47	100.00
Wavelength λ (Å)	1.54	1.54	1.54	1.54
Crystal Size D (nm)	28.485	24.919	24.919	33.389
Average Crystal Size (nm)	26.233	26.233	26.233	26.233

The width of peaks attributes the anisotropic crystallite size and the diffraction spectrum consisting the sharp and wide peaks reveals heterogeneous crystallite sizes of the prepared nanocomposite. It is observed that the sharp peaks at 38.4° , 44.6° , 72.6° and 77.7° positions are due to most crystalline crystals while less ordered crystal found in 25.6° , 42.5° and 65° [23].

It clears that the peaks were shifted toward higher values of 2θ which means that the interlayer spacing is smaller than the reference peaks of hematite. [24]. There are some peaks missing which implies that impurity phases are present in the composite at any step during its preparation. [25].

3.2 FTIR:

The surface functional groups were found as a contamination in the synthesized composite is characterized by Fourier Transform Infrared (FT-IR) spectroscopy. The FTIR spectrum of the

composite is shown in the figure.2. The spectrum indicates absorption peaks of 3919, 3879, 3839, 3753, 3688, 3474, 3417, 2829, 2852, 2030, 1637, 630, 476 and 422 cm^{-1} . The group frequency assigned to their corresponding functional group is given in table 2.

The presence of frequency ranges between 400-560 cm^{-1} implies the Fe II-O stretching bond which in turn characterizes the hematite. [26] The peak ranges 570 -702 cm^{-1} were different from maghemite and magnetite and the group lying between 3200-3570 acknowledged to the adsorbed water [28] and the band 3570 - 3200 cm^{-1} confirms the OH functionalized CNT which is wideband, reflecting a large number of OH attached to MWCNT [22]. The band between the range 1690-1590 cm^{-1} were assigned to the hexagonal Sp^2 C=C bonding and also the C=O stretching between 1700-2100 cm^{-1} in the MWCNT [29].

Table 2: Functional Groups with IR frequency ranges

Group frequency (cm^{-1})	Functional group/ions
400-560	FeII-O stretching
705-570	FeII-O stretching
1690-1590	CNT
2100-1700	Transition metal carbonyl
2945-2865	Methylene (C-H) symmetric stretch
2935-2915	Methylene (C-H) antisymmetric stretch
3570-3200	Hydroxy group, H-bonded OH stretch

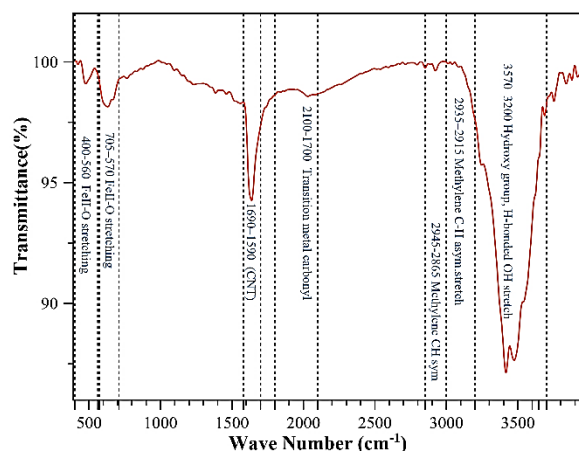


Figure 2: FTIR Spectrum with various functional groups

3.3 SEM:

The surface morphology was investigated by Scanning electron microscope SEM at different magnifications and scales. It sees that in the figures 3,4,5 and 6. The particles of hematite like sphere were maintained on the surface of CNT due to the hydrophobicity of CNT and they are

polycrystalline in nature due to the wet chemical approach and also long needle-like structures represent the MWCNTs [30][31]. Hematite leads to non-uniform dispersion of CNTs in the structure and shows agglomeration in the form of bundles [32].

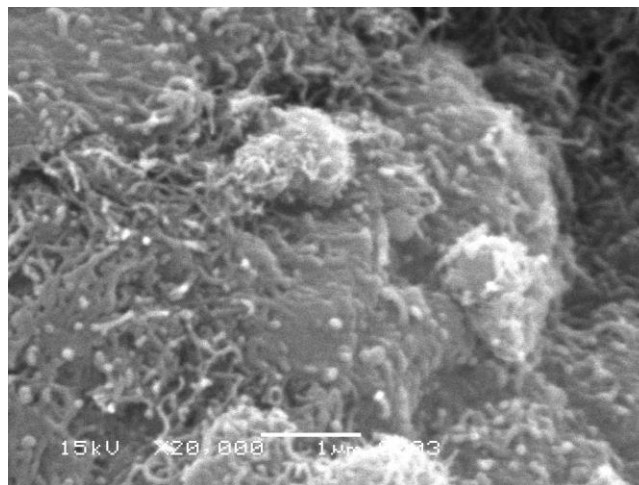


Figure 3: SEM image taken at 1 um and 20000 magnification

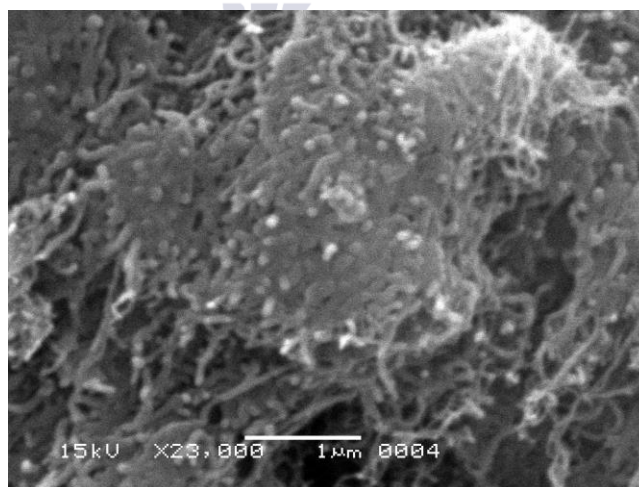


Figure 4: SEM image at 1 um scale and 23000 magnification

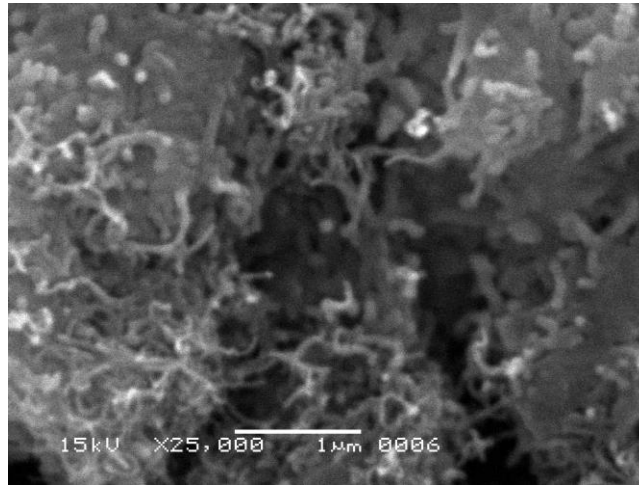


Figure 5: SEM image at 1 μm scale and 25000 magnification

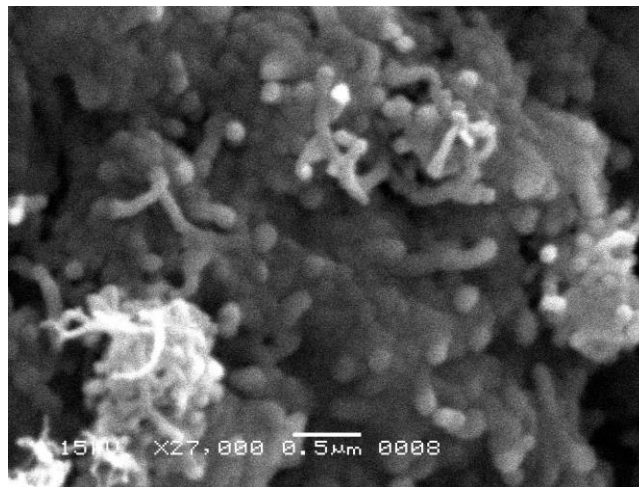


Figure 6: SEM image at 1 μm scale and 25000 magnification

3.4 VSM:

Magnetic properties of the synthesized nanocomposite were studied by Micro Sense Easy VSM. The applied magnetic field was between 1.2 T to -1.2 T. The observed saturation magnetization (Ms), Remnant magnetization (Mr), coercivity (Hc) for the hematite/CNT nanocomposite were obtained 1.2 (emu/g), 0.5(emu/g) and 0.02 tesla (200 Oersted) as shown in the figure 4.7(a),(b). In a

comparison of Multi-Wall CNT these values of coercivity, saturation magnetization and large magnetic susceptibility were due to the decoration of hematite on the outside of CNT and are different from the super magnetic inner filled nanocomposite and the composite exhibits ferromagnetism [32][27][33] and implying smaller particle size and morphology of hematite as compare to the bulk iron [34].

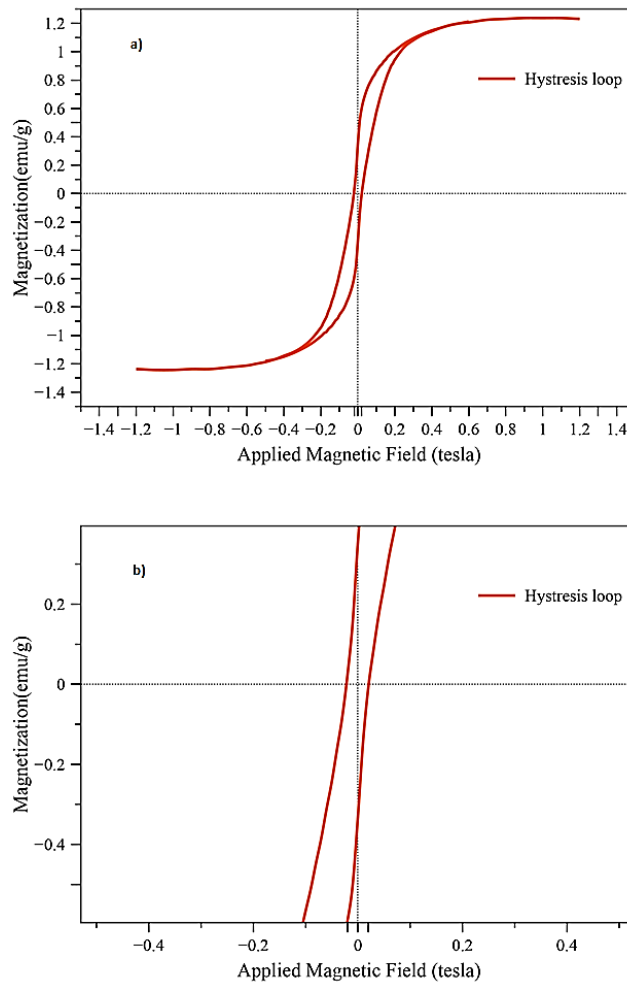


Figure 8: Magnified view of hysteresis loop

Authors Contribution

Author 1: Formal analysis Software, Visualization, Writing - original draft

Author 2: Investigation Project administration, Resources

Author 3: Conceptualization, Data curation, Funding acquisition, Methodology, Supervision Validation, Writing - review & editing

Conflicts of Interest

All authors declare that they have no conflicts of interest.

Acknowledgment

I am deeply thankful to our university for giving an opportunity along with to some people, who

worked hard with me from the starting till the completion of the present research particularly my supervisor Dr. Syed Farhan Hasany, who has been substantial of all research phases and without her support and encouragement this study would not have been possible, and I highly appreciate the efforts expended by my co-supervisor Mr. Syed Ghazanfar Hussain. I would also like to thanks my chairperson for this opportunity. I would like to take this chance to say warm thanks to all my beloved friends and my Vice principle and Vice Principle (Bahria College, Karim Campus), who have been so supportive in my research work and along the way of doing my thesis. I owe profound gratitude to my Father & Mother (Parents), whose

constant inspiration and limitless helped me to accomplish my degree.

DANISH RAZA

Data Availability statement

The data presented in this study are available on request from the corresponding author.

4. Conclusion:

The Chemical wet approach is simple, cost effective and reproducible. Like Hematite many other metals could be decorated on the surface of CNT by this convenient way. Characterization data implies that the synthesized nanohybrid is a suitable material to be used in the electrodes of Lithium-ion battery and super capacitor.

Authors bibliography

I, **Danish Raza**, pursued M.S Degree from NED University of Engineering & Technology, Karachi. And is a Ph.D. Scholar at COMSATS University, Islamabad

Sajid Hussain, PhD Scholar, Assistant Professor, Institute of Industrial Electronics Engineering, Karachi.

Syed Farhan Hasany, Researcher, Assistant Professor, NED University of Engineering & Technology, Karachi

REFERENCES

- [1] M. E. Franke, T. J. Koplín, and U. Simon, "Metal and metal oxide nanoparticles in chemiresistors: Does the nanoscale matter?," *Small*, vol. 2, no. 1, pp. 36–50, 2006, doi: 10.1002/sml.200500261.
- [2] S. Brovelli, N. Chiodini, R. Lorenzi, A. Lauria, M. Romagnoli, and A. Paleari, "Fully inorganic oxide-in-oxide ultraviolet nanocrystal light emitting devices," *Nat. Commun.*, vol. 3, no. 1, p. 690, Jan. 2012, doi: 10.1038/ncomms1683.
- [3] A. Stein, "Batteries take charge," *Nat. Nanotechnol.*, vol. 6, no. 5, pp. 262–263, May 2011, doi: 10.1038/nnano.2011.69.
- [4] H. Woo et al., "Azide-Alkyne Huisgen [3+2] Cycloaddition Using CuO Nanoparticles," *Molecules*, vol. 17, no. 11, pp. 13235–13252, Nov. 2012, doi: 10.3390/molecules171113235.
- [5] S. F. Hasany, I. Ahmed, R. J., and A. Rehman, "Systematic Review of the Preparation Techniques of Iron Oxide Magnetic Nanoparticles," *Nanosci. Nanotechnol.*, vol. 2, no. 6, pp. 148–158, 2013, doi: 10.5923/j.nn.20120206.01.
- [6] Y. Tan, X. Dai, Y. Li, and D. Zhu, "Preparation of gold, platinum, palladium and silver nanoparticles by the reduction of their salts with a weak reductant–potassium bitartrate," *J. Mater. Chem.*, vol. 13, no. 5, pp. 1069–1075, Apr. 2003, doi: 10.1039/b211386d.
- [7] J. Turkevich, P. C. Stevenson, and J. Hillier, "A study of the nucleation and growth processes in the synthesis of colloidal gold," *Discuss. Faraday Soc.*, vol. 11, p. 55, 1951, doi: 10.1039/df9511100055.
- [8] Y. Nagasaki, "Engineering of poly(ethylene glycol) chain-tethered surfaces to obtain high-performance bionanoparticles," *Sci. Technol. Adv. Mater.*, vol. 11, no. 5, p. 054505, Oct. 2010, doi: 10.1088/1468-6996/11/5/054505.
- [9] M. Brust, M. Walker, D. Bethell, D. J. Schiffrin, and R. Whyman, "Synthesis of thiol-derivatised gold nanoparticles in a two-phase Liquid–Liquid system," *J. Chem. Soc., Chem. Commun.*, no. 7, pp. 801–802, 1994, doi: 10.1039/C39940000801.
- [10] I. Pastoriza-Santos and L. M. Liz-Marzán, "Formation and Stabilization of Silver Nanoparticles through Reduction by N,N-Dimethylformamide," *Langmuir*, vol. 15, no. 4, pp. 948–951, Feb. 1999, doi: 10.1021/la980984u.
- [11] K. L. Tsai and J. L. Dye, "Synthesis, properties, and characterization of nanometer-size metal particles by homogeneous reduction with alkalides and electrides in aprotic solvents," *Chem. Mater.*, vol. 5, no. 4, pp. 540–546, Apr. 1993, doi: 10.1021/cm00028a023.
- [12] K. L. Tsai and J. L. Dye, "Nanoscale metal particles by homogeneous reduction with alkalides or electrides," *J. Am. Chem. Soc.*, vol. 113, no. 5, pp. 1650–1652, Feb. 1991, doi: 10.1021/ja00005a031.

- [13] J. Miao and B. Liu, "II-VI semiconductor nanowires: ZnO," *Semicond. Nanowires Mater. Synth. Charact. Appl.*, pp. 3–28, 2015, doi: 10.1016/B978-1-78242-253-2.00001-3.
- [14] H. Bönemann et al., "Wet Chemistry Synthesis of β -Nickel Aluminide NiAl," *Angew. Chemie Int. Ed.*, vol. 41, no. 4, pp. 599–603, Feb. 2002, doi: 10.1002/1521-3773(20020215)41:4<599::AID-ANIE599>3.0.CO;2-R.
- [15] H. Bönemann et al., "A size-selective synthesis of air stable colloidal magnetic cobalt nanoparticles," *Inorganica Chim. Acta*, vol. 350, pp. 617–624, Jul. 2003, doi: 10.1016/S0020-1693(03)00108-7.
- [16] G. Viau et al., "Ruthenium Nanoparticles: Size, Shape, and Self-Assemblies," *Chem. Mater.*, vol. 15, no. 2, pp. 486–494, Jan. 2003, doi: 10.1021/cm0212109.
- [17] M. T. Reetz and W. Helbig, "Size-Selective Synthesis of Nanostructured Transition Metal Clusters," *J. Am. Chem. Soc.*, vol. 116, no. 16, pp. 7401–7402, Aug. 1994, doi: 10.1021/ja00095a051.
- [18] L. Rodríguez-Sánchez, M. C. Blanco, and M. A. López-Quintela, "Electrochemical Synthesis of Silver Nanoparticles," *J. Phys. Chem. B*, vol. 104, no. 41, pp. 9683–9688, Oct. 2000, doi: 10.1021/jp001761r.
- [19] M. B. Mohamed, Z. L. Wang, and M. A. El-Sayed, "Temperature-Dependent Size-Controlled Nucleation and Growth of Gold Nanoclusters," *J. Phys. Chem. A*, vol. 103, no. 49, pp. 10255–10259, Dec. 1999, doi: 10.1021/jp9919720.
- [20] A. V. Nikam, B. L. V. Prasad, and A. A. Kulkarni, "Wet chemical synthesis of metal oxide nanoparticles: A review," *CrystEngComm*, vol. 20, no. 35, pp. 5091–5107, 2018, doi: 10.1039/C8CE00487K.
- [21] S. F. Hasany, N. H. Abdurahman, A. R. Sunarti, and A. Kumar, "Non-covalent assembly of maghemite-multiwalled carbon nanotubes for efficient lead removal from aqueous solution," *Aust. J. Chem.*, vol. 66, no. 11, pp. 1440–1446, 2013, doi: 10.1071/CH13281.
- [22] Chap 2. Characterization of MWCNT.
- [23] J. C. Hulteen, D. A. Treichel, M. T. Smith, M. L. Duval, T. R. Jensen, and R. P. Van Duyne, "Nanosphere lithography: Size-tunable silver nanoparticle and surface cluster arrays," *J. Phys. Chem. B*, vol. 103, no. 19, pp. 3854–3863, 1999, doi: 10.1021/jp9904771.
- [24] M. A. Alaa, K. Yusoh, and S. F. Hasany, "Synthesis and characterization of polyurethane-organoclay nanocomposites based on renewable castor oil polyols," *Polym. Bull.*, vol. 72, no. 1, pp. 1–17, 2014, doi: 10.1007/s00289-014-1255-6.
- [25] A. B. R. Ghosh, Narendra Nath, "Preparation of Polybenzoxazine-Ni-Zn Ferrite Nanocomposites and Their Magnetic Property," in *Handbook of Benzoxazine Resins*, Elsevier, 2011, pp. 641–650. doi: 10.1016/B978-0-444-53790-4.00082-5.
- [26] S. Mohammed and H. Mohammed, "Characterization of Magnetite and Hematite Using Infrared Spectroscopy," vol. 83, no. 1, doi: 10.26389/AJSRP.S110318.
- [27] F. Zhao, H. Duan, W. Wang, and J. Wang, "Synthesis and characterization of magnetic Fe / CNTs composites with controllable Fe nanoparticle concentration," *Phys. B Phys. Condens. Matter*, vol. 407, no. 13, pp. 2495–2499, 2012, doi: 10.1016/j.physb.2012.03.052.
- [28] D. Zhao, X. Wang, S. Yang, Z. Guo, and G. Sheng, "Impact of water quality parameters on the sorption of U(VI) onto hematite," *J. Environ. Radioact.*, vol. 103, no. 1, pp. 20–29, 2012, doi: 10.1016/j.jenvrad.2011.08.010.
- [29] J. Z. Chao Xu, Xin Wang and Key, "Graphene-metal particle nanocomposites," Nanjing.
- [30] S. F. Hasany, N. H. Abdurahman, and A. R. Sunarti, "Wet chemical for vanadium doped meghmemite Nanocrystals," no. 3, pp. 617–620, 2016, doi: 10.2174/15734137126661603.

- [31] S. L. Chou, J. Z. Wang, Z. X. Chen, H. K. Liu, and S. X. Dou, "Hollow hematite nanosphere/carbon nanotube composite: Mass production and its high-rate lithium storage properties," *Nanotechnology*, vol. 22, no. 26, 2011, doi: 10.1088/0957-4484/22/26/265401.
- [32] L. Jiang and L. Gao, "Carbon Nanotubes - Magnetite Nanocomposites from Solvothermal Processes: Formation, Characterization, and Enhanced Electrical Properties," no. 15, pp. 2848-2853, 2003.
- [33] Z. Sun, Z. Liu, Y. Wang, B. Han, J. Du, and J. Zhang, "Fabrication and characterization of magnetic carbon nanotube composites," pp. 4497-4501, 2005, doi: 10.1039/b509968d.
- [34] W. Wu, Z. Wu, T. Yu, C. Jiang, and W.-S. Kim, "Recent progress on magnetic iron oxide nanoparticles: synthesis, surface functional strategies and biomedical applications," *Sci. Technol. Adv. Mater.*, vol. 16, no. 2, p. 023501, Apr. 2015, doi: 10.1088/1468-6996/16/2/023501.

